Journal of Power Sources 196 (2011) 4865–4869

Contents lists available at ScienceDirect

Journal of Power Sources

journal homepage: www.elsevier.com/locate/jpowsour

Short communication

Single-step fabrication of phase-controllable nanocrystalline TiO_2 films for enhanced photoelectrochemical water splitting and dye-sensitized solar cells

Chin-Jung Lin[a], Wen-Kai Tu[b], Chih-Kang Kuo[b,c], Shu-Hua Chien[b,c,*]

[a] Department of Environmental Engineering, National I-Lan University, Taiwan
[b] Institute of Chemistry, Academia Sinica, Taipei 11529, Taiwan
[c] Department of Chemistry, National Taiwan University, Taipei 10617, Taiwan

ARTICLE INFO

Article history:
Received 2 September 2010
Received in revised form 8 December 2010
Accepted 21 December 2010
Available online 7 January 2011

Keywords:
Phase-controllable TiO_2 film
Single-step fabrication
Photoelectrochemical water splitting
Dye-sensitized solar cell

ABSTRACT

We introduce a single-step procedure for growing a phase-controllable bilayer-structured TiO_2 film directly onto transparent conductive oxide glass by precipitation from hydrolysis of $TiCl_4$ in acid solution containing sulfate ions. The obtained bilayer-structured film with anatase nanoparticles in the inner layer which provide high surface area, and an outer layer of larger rutile particles for incident light scattering. In both the water splitting and the dye-sensitized solar cells under AM 1.5 simulated solar light, the bilayer-structured film outperformed the single layer-structured films with either anatase or rutile TiO_2 alone by at least 50%.

1. Introduction

Significant attention has been given to photoelectrochemical water splitting and dye-sensitized solar cells (DSSCs) using semiconducting metal-oxide films (e.g., TiO_2, ZnO, WO_3, and Fe_2O_3) to supply clean and recyclable energy [1–4]. Of the materials being developed for photoanode, titania (TiO_2) is the most promising because of its low cost and photochemical stability [5,6]. To develop more efficient TiO_2 films, considerable efforts have been made mostly to overcome the recombination of photoexcited carriers by either replacing a random TiO_2 nanoparticle network with an ordered TiO_2 film [7–9] or using core-shell structures with an oxide coating on TiO_2 [10,11]. Besides these approaches, an effective method that addresses the generation of photoexcited carriers by adding a light-scattering layer over nanocrystalline TiO_2 film has been demonstrated to elongate path length of incident light within the films, thereby enhancing the light-harvesting capability of the electrode film and the performance of photoelectrochemical devices [12–16]. In the fabrication of electrode films, sintering of a binder-containing TiO_2 paste [12–14], and electrophoretic deposition of TiO_2 particles [17–19] are mostly used. In both techniques, the nanocrystalline TiO_2 particle layers are repeatedly deposited onto a transparent conducting oxide (TCO) glass substrate to a desired thickness and the light-scattering layers of submicron TiO_2 particles are then printed atop these films. These time- and energy-consuming layer-by-layer TiO_2-coating procedures are tedious for practical use. A facile route of mesoporous TiO_2 film fabrication for high-performance photoelectrochemical devices still remains a challenge.

Utilization of hydrolyzed organic or inorganic titanium precusor for directly depositing TiO_2 films onto TCO glasses [20,21] is currently alternative to the repetitive layer-by-layer assembly technique, although other methods relied on vapor phase syntheses [22–24] for mesoporous films are available. Compared to vapor phase techniques, the solution routes of hydrolyzed titanium precusors are more suitable for inexpensive mass production. But only the single-layered film containing either anatase or rutile TiO_2 alone has been reported to date [20,21]. In this study, a single-step procedure for growing phase-controllable TiO_2 particles in continuous films directly onto TCO glass via the hydrolysis of $TiCl_4$ in acid solution containing sulfate ions is reported for the first time. Remarkably improved performances of photoelectrochemical water splitting and dye-sensitized solar cells under AM 1.5 solar light were evident as compared with the single-layered film containing either anatase or rutile TiO_2 alone.

2. Experimental

For understanding the influence of sulfate ions on the phase evolution in TiO_2 during $TiCl_4$ hydrolysis, the *in situ* XRD experiments were performed using a synchrotron X-ray source at the

* Corresponding author at: Institute of Chemistry, Academia Sinica, Taipei 11529, Taiwan. Tel.: +886 2 27898528; fax: +886 2 27831237.
E-mail address: chiensh@gate.sinica.edu.tw (S.-H. Chien).

0378-7753/$ – see front matter © 2011 Elsevier B.V. All rights reserved.
doi:10.1016/j.jpowsour.2010.12.077

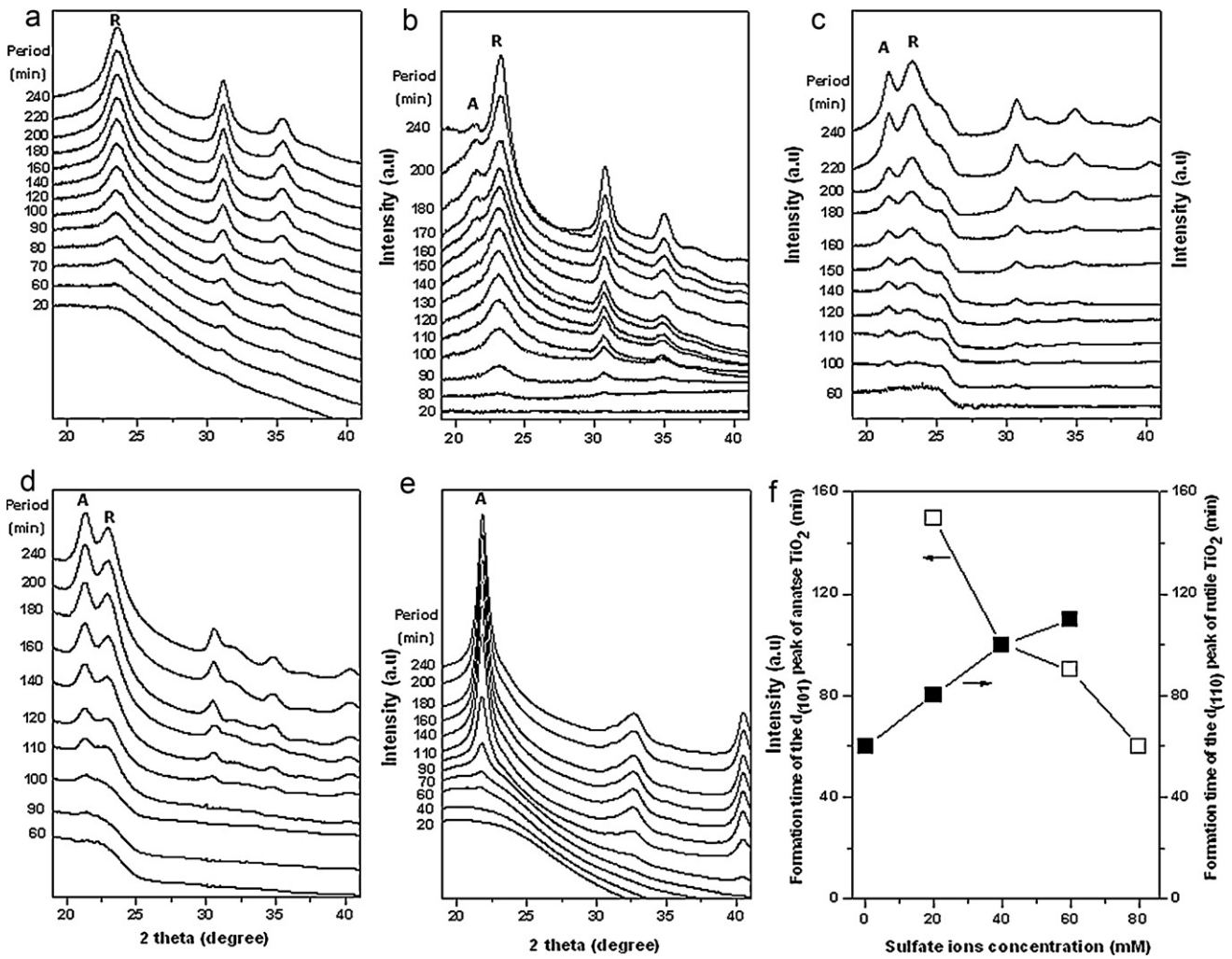

Fig. 1. *In situ* XRD patterns using a synchrotron X-ray radiation source (λ = 0.134431 nm) of TiO_2 formed in the $TiCl_4/HNO_3$ hydrothermal systems with (a) 0 mM, (b) 20 mM, (c) 40 mM, (d) 60 mM, and (e) 80 mM sulfate ions. (f) The time of first appearance of the characteristic peaks of anatase and rutile TiO_2 (A and R refer to anatase and rutile phase).

National Synchrotron Radiation Research Center facility in Taiwan. The synchrotron X-ray radiation wavelength (λ) was 1.334431 Å. The solutions containing 5 M HNO_3, 0.6 M $TiCl_4$, and various sulfate ion concentrations were separately prepared and sealed in quartz capillaries (outer diameter: 1 mm, length: 80 mm, and wall thickness: 0.01 mm). The reaction temperature was maintained at 100 °C by a gas-flow heater. *In situ* XRD data were collected by image plate detection (192 s exposure time for each spectrum taken).

In the fabrication of TiO_2 film electrodes, each FTO glass substrate (2 cm × 3 cm) was cleaned with ethanol under ultrasonic treatment and then immersed into the solutions containing 5 M HNO_3, 0.6 M $TiCl_4$ and various sulfate ion concentrations at 100 °C for 4 h. The resulting films deposited onto the FTO glasses were rinsed with distilled water and dried for 30 min in an oven at 120 °C. The obtained TiO_2 films were characterized by X-ray diffraction (XRD, SIEMEMS D500 X-ray diffractometer with Cu Kα radiation of 1.54 Å), field-emission scanning electron microscopy (FE-SEM, LEO 1530).

Photoelectrochemical water splitting experiments were conducted using a three-electrode configuration with a Pt wire counter electrode and a saturated Ag/AgCl reference electrode. The electrolyte was a 1 M KOH solution. The three working electrodes of the TiO_2 film/FTO were illuminated with an AM 1.5 Class A solar simulator (Oriel) during a voltage sweep from −1.0 to 0.6 V (vs. Ag/AgCl) with a sweep rate of 5 mV s^{-1}.

For use in the DSSCs, each photoanode was immersed into 0.3 mM $(Bu_4N)_2[Ru(dcbpyH)_2\text{-}(NCS)_2]$ (N719 dye, Solaronix) solution for 24 h. The N719-sensitized electrode was further sandwiched with the sputtered-Pt FTO glass, separated by a 25 μm thick hot-melt spacer. The intervening space was filled with liquid electrolytes of 0.5 M LiI, 0.05 M I_2, and 0.5 M tert-butylpyridine in dry acetonitrile. Photocurrent–photovoltage (*I–V*) characteristics of the DSSCs were measured using an electrochemical analyzer (650B, CH Instruments) under AM 1.5 solar light illumination at an intensity of 100 mW cm^{-2}. The N719 dye adsorption measurements were done by dissolving it completely from the sensitized films into a 0.2 M NaOH solution. Concentrations of N719 dye were determined by UV–Vis spectroscopy (U-3410, Hitachi).

3. Results and discussion

In situ XRD spectra of the titania formed from the $TiCl_4/HNO_3$ hydrothermal system with various sulfate ion concentrations are shown in Fig. 1(a)–(e). It clearly indicates that pure rutile phase was formed without the addition of sulfate ions and pure anatase phase was obtained at 80 mM sulfate ions. Other samples turned out to be a mixture of anatase and rutile phase and the increase in the sulfate ion concentration resulted in more anatase phase as reported by Yan et al. [25]. The influence of sulfate ion concentration on the time (designated as *t*) needed for the first appearance of the

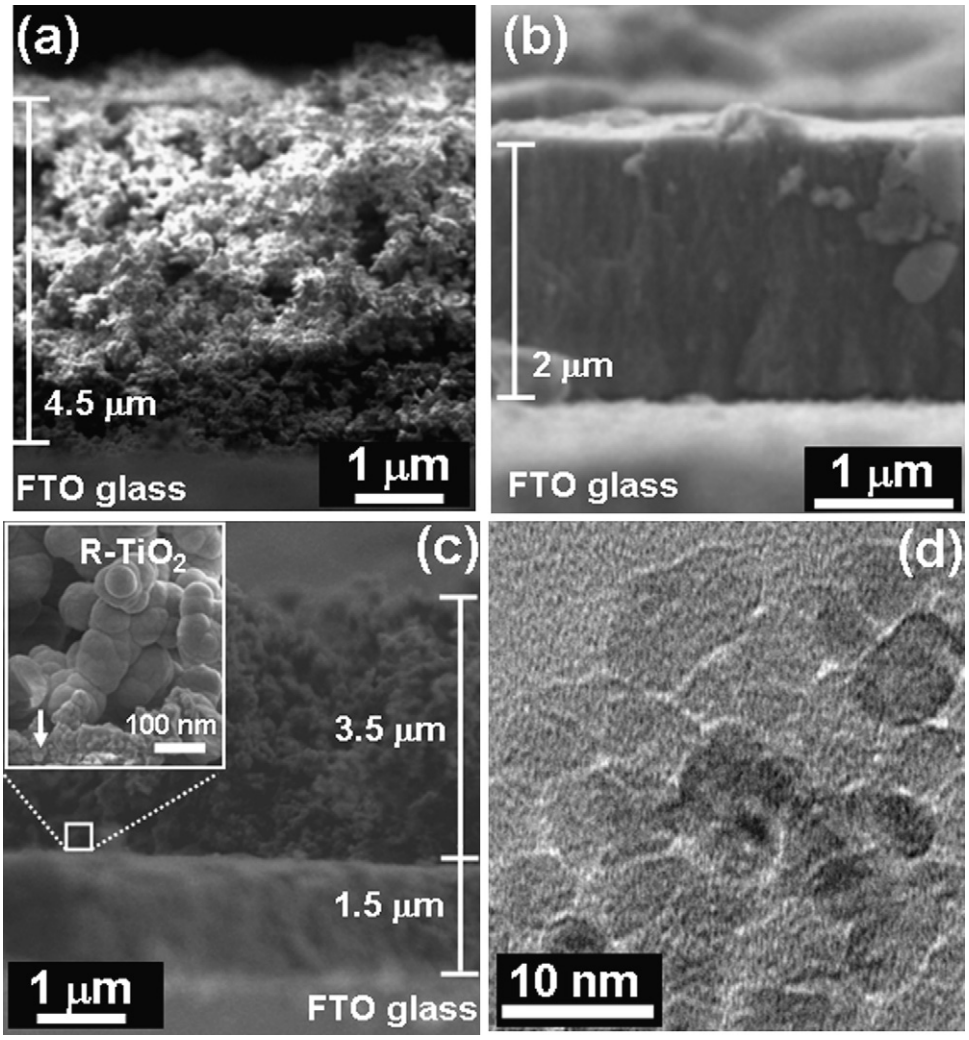

Fig. 2. Side-view FE-SEM images of TiO_2 films on FTO glass prepared in the $TiCl_4/HNO_3$ hydrothermal systems with (a) 0 mM, (b) 80 mM, and (c) 60 mM sulfate ions. (d) The TEM image of small TiO_2 particles in (c) sample.

characteristic peaks of anatase or rutile TiO_2 is shown in Fig. 1(f). With an increase in sulfate ion concentration in the $TiCl_4/HNO_3$ hydrothermal system, the *t* value of anatase TiO_2 gradually dropped and lowered to about 60 min when 80 mM of sulfate ions was added. In contrast, the *t* value of rutile TiO_2 rose markedly by adding sulfate ions. With an increase to 80 mM of sulfate ions, characteristic peaks of rutile TiO_2 did not appear even when reaction time was prolonged to 24 h. These results demonstrate that the increase in sulfate ion concentration in the $TiCl_4/HNO_3$ hydrothermal system would accelerate the formation of anatase TiO_2 and retard the rutile TiO_2 formation. The above experiments gave us a useful guide for the direct growth of phase-controlled TiO_2 film onto the TCO glass.

Fig. 2(a)–(c) is the FE-SEM images with side views of TiO_2 films deposited onto the FTO glasses in the $TiCl_4/HNO_3$ hydrothermal systems with 0, 80 and 60 mM sulfate ions, respectively. As shown in Fig. 2(a) and (b), the 4.5 μm thick and 2.0 μm thick single-layered films were formed with 0 and 80 mM sulfate ions, respectively, and significant differences in the morphology and particle size between them were observed. Without addition of sulfate ions, large deposited particles were randomly packed and loosely interconnected on top of the FTO glass. Small particles were well-adhered to and compactly arranged on the FTO glass in the synthesis system with 80 mM sulfate ions. With addition of 60 mM sulfate ions, the titania film appeared clearly to be a bilayered structure with a 3.5 μm thick outer layer of large TiO_2 particles and a 1.5 μm thick inner layer of compact TiO_2 particles. The outer layer consisted of 100–150 nm TiO_2 particles mixed with a small amount of 10–20 nm TiO_2 nanoparticles, as can be seen in the inset of Fig. 2(c) and (d), respectively. The XRD spectra in Fig. 3 show that the TiO_2 films crystallized as pure rutile, pure anatase, and mixed rutile/anatase phases when prepared in synthesis systems without the addition of sulfate ions and with 80 and 60 mM sulfate ions, respectively. Accordingly, the bilayer-structured film was composed of two distinct layers with a mixed rutile/anatase TiO_2 outer layer atop the anatase TiO_2 inner layer. These three types of films were designated as A-TiO_2/FTO, R-TiO_2/FTO, and R/A-TiO_2/FTO. Three types of TiO_2 films were chosen, including the pure anatase, the pure rutile, and the mixed anatase/rutile films, for the direct deposition of nanocrystalline TiO_2 films onto the FTO glasses.

In the photoelectrochemical water splitting experiments, the photocurrent densities generated from these three photoanodes are presented in Fig. 4(a). Obviously, the photocurrent generated with the R/A-TiO_2 film/FTO is higher than those of the A-TiO_2 film/FTO and R-TiO_2 film/FTO. Photoconversion efficiency (η) of the transformation of light energy to chemical energy in the presence of an externally applied potential is calculated according to: $\eta(\%) = j_p[(E^o_{rev} - E_{app})/I_0] \times 100$, where E^o_{rev} equals 1.23 V, $E_{app} = E_{meas} - E_{ocp}$, j_p is the photocurrent density, and I_0 is the intensity of the incident light. The term E_{meas} is the electrode potential (vs. Ag/AgCl) of the photoanode. The results are depicted in Fig. 4(b).

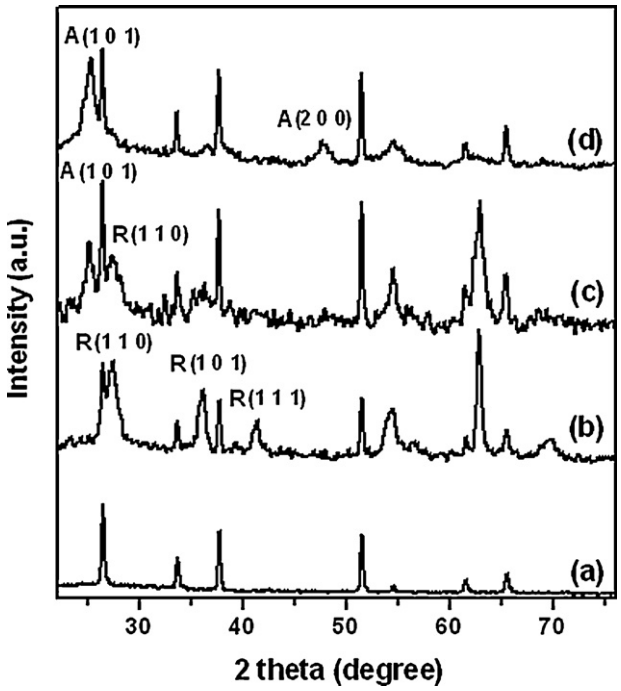

Fig. 3. XRD spectra of (a) blank FTO glass, and the TiO_2 films on FTO glass prepared in the $TiCl_4/HNO_3$ hydrothermal systems with (b) 0 mM, (c) 60 mM, and (d) 80 mM sulfate ions (A and R refer to anatase and rutile phase).

A maximum energy conversion efficiency up to 0.41% was achieved using the bilayered TiO_2/FTO, which was much higher than the 0.15% efficiency obtained by the anatase TiO_2/FTO or the 0.27% efficiency by the rutile TiO_2/FTO electrode.

The *I–V* characteristics for the three DSSCs are presented in Fig. 5, and the measured cell parameters are presented in Table 1. The anatase transparent layer-only (A-TiO_2/FTO) cell fabricated without a scattering layer exhibited an short-circuit photocurrent density (I_{sc}) of 6.5 mA cm^{-2}. After growing a scattering layer atop the anatase TiO_2 layer (R/A-TiO_2/FTO), I_{sc} was dramatically increased up to 10.3 mA cm^{-2}; as compared to I_{sc} of 2.5 mA cm^{-2} for the rutile layer-only (R-TiO_2/FTO), 66% of the improvement was due to the rutile scattering layer fabricated over the anatase transparent layer. Dye loadings, determined by dye desorption, were 0.004 μmol cm^{-2} in the rutile TiO_2 film, 0.020 μmol cm^{-2} in the anatase TiO_2 film, and 0.022 μmol cm^{-2} in the bilayered film. The difference in dye loadings between both the A-TiO_2/FTO-based and the R/A-TiO_2/FTO-based cells was not significant. Accordingly, the higher current in the R/A-TiO_2/FTO-based cell was primar-

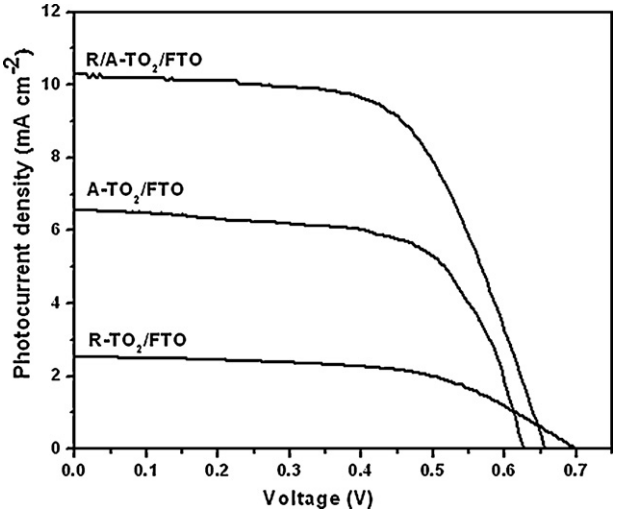

Fig. 5. *I–V* curves for dye-sensitized solar cells based on the photoanodes of R-TiO_2 film/FTO, A-TiO_2 film/FTO, and R/A-TiO_2 film/FTO glasses.

Table 1
The photovoltaic properties of dye-sensitized solar cells based on the photoanodes of R-TiO_2/FTO, A-TiO_2/FTO, and R/A-TiO_2/FTO glasses.

Photoanode	$N719_{ads}$ (μmol cm^{-2})	V_{oc} (V)	I_{sc} (mA cm^{-2})	FF	η (%)
R-TiO_2/FTO	0.004	0.7	2.5	0.57	1.00
A-TiO_2/FTO	0.020	0.63	6.5	0.64	2.65
R/A-TiO_2/FTO	0.022	0.66	10.3	0.60	4.08

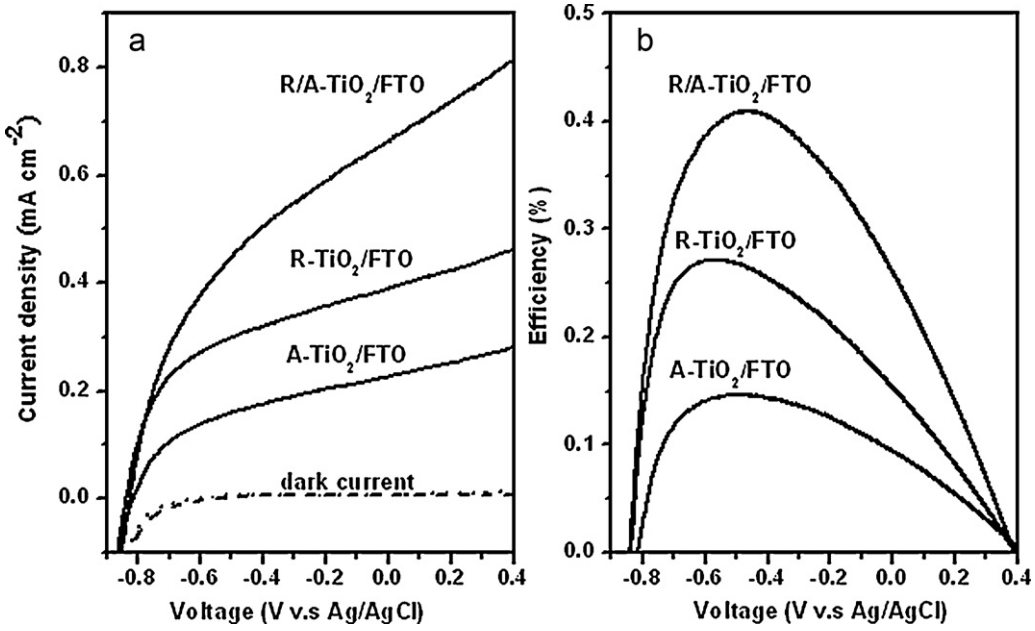

Fig. 4. (a) Current density–potential characteristics for water splitting using the A-TiO_2 film/FTO glass, the R-TiO_2 film/FTO glass, and the R/A-TiO_2 film/FTO glass in the dark and under AM 1.5 illumination. (b) The corresponding photoconversion efficiencies.

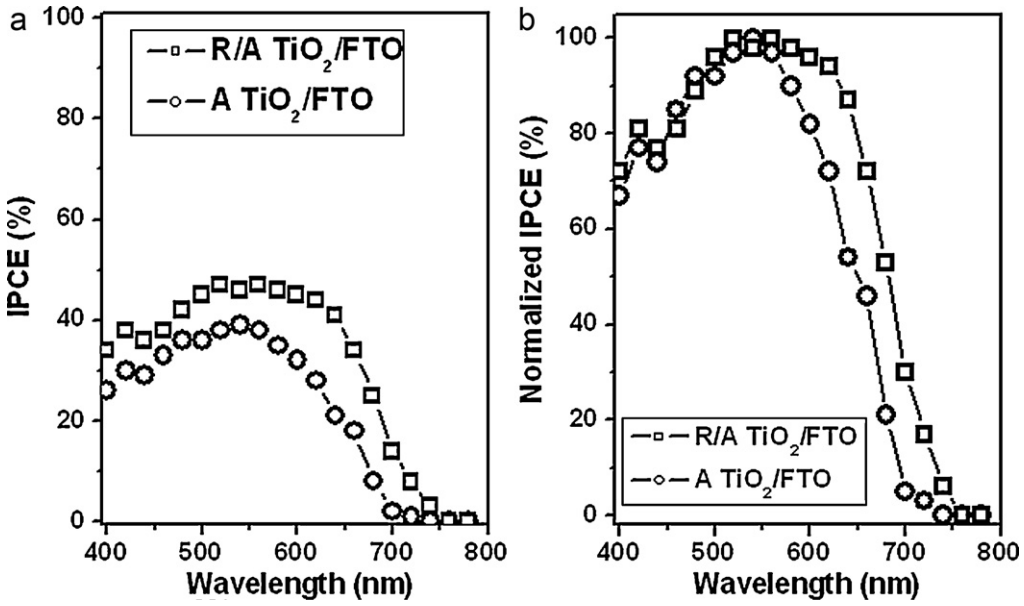

Fig. 6. (a) Measured IPCE spectra of the A-TiO_2 film/FTO-based DSSC (circle symbol) and the R/A-TiO_2 film/FTO-based DSSC (square symbol); (b) The data of (a) are normalized by the intensity of the 560 nm peak.

ily due to light scattering, rather than light absorbed within the scattering layer that was confirmed by IPCE measurements (described in the below section). A solar conversion efficiency of 4.1% was obtained by the R/A-TiO_2/FTO film without sufficient optimization.

The IPCE of the A-TiO_2/FTO-based and the R/A-TiO_2/FTO-based DSSCs are depicted in Fig. 6(a). Although the dye coverage of the A-TiO_2/FTO and the R/A-TiO_2/FTO electrodes were similar, a significant enhancement of the IPCE in full spectrum for the R/A-TiO_2/FTO-based cell was observed. Fig. 6(b) shows IPCE data normalized to the intensity of 560 nm peak. The relatively high IPCE values of the R/A-TiO_2/FTO electrode at the long-wavelength side of the peak maximum are attributed to the enhanced light harvesting within the electrode. This is due to the rutile upper layer provides the scattering center for incident light, thus elongating the path-length of the long-wavelength incident light to promote the capture of photons by dye molecules. Therefore, the enhanced light-confinement performance resulted in a higher I_{sc}. Further enhancement of the photoelectrochemical performance is expected to be achieved through thickening the anatase transparent layer and thinning the rutile scattering layer by controlling the addition of sulfate ions.

4. Conclusions

The direct growth of a phase-controllable TiO_2 film onto the FTO glass was successfully achieved by precipitation from hydrolyzed $TiCl_4$ solution in the presence of sulfate ions. Either a single layer- or a bilayer-structured TiO_2 film can be obtained by changing sulfate ion concentrations in the hydrothermal systems. The performance of these films was tested in two different devices, water splitting and DSSCs. For both devices, the bilayer-structured film outperformed the monolayer-structured films by at least 50%. This facile, scalable and substrate-independent preparation process of phase-controllable TiO_2 film will open up an alternative route for the development of low-cost and high-performance photoelectrochemical devices.

Acknowledgements

We acknowledge the financial supports from Academia Sinica and National Science Council of Taiwan, and the utilization of the beam line in the National Synchrotron Radiation Research Center (NSRRC) in Taiwan.

References

[1] B. O'Regan, M. Grätzel, Nature 353 (1991) 737.
[2] A.B. Murphy, P.R.F. Barnes, L.K. Randeniya, I.C. Plumb, I.E. Grey, M.D. Horne, J.A. Glasscock, Int. J. Hydrogen Energy 31 (2006) 1999.
[3] Y.S. Hu, A. Kleiman-Shwarsctein, A.J. Forman, D. Hazen, J.N. Park, E.W. McFarland, Chem. Mater. 20 (2008) 3803.
[4] K.S. Ahn, S. Shet, T. Deutsch, C.S. Jiang, Y. Yan, M. Al-Jassim, J. Yurner, J. Power Sources 176 (2008) 387.
[5] A.L. Linsebigler, G. Lu, J.T. Yates, Chem. Rev. 95 (1995) 735.
[6] C. Burda, Y. Lou, X. Chen, A.C.S. Samia, J. Stout, J.L. Gole, Nano Lett. 3 (2003) 1049.
[7] W. Chen, X. Sun, Q. Cai, D. Weng, H. Li, Electrochem. Commun. 9 (2007) 382.
[8] C.J. Lin, W.Y. Yu, Y.T. Lu, S.H. Chien, Chem. Commun. (2008) 6031.
[9] A.S. Nair, R. Jose, Y. Shengyuan, S. Ramakrishna, J. Colloid Interface Sci. 353 (2010) 39.
[10] Y. Yin, Z. Jin, F. Hou, Nanotechnology 18 (2007) 495608.
[11] C.J. Lin, Y.T. Lu, C.H. Hsieh, S.H. Chien, Appl. Phys. Lett. 94 (2009) 113102.
[12] C.J. Barbé, F. Arende, P. Comet, M. Jirousek, F. Lenzmann, V. Shklover, M. Grätzel, J. Am. Ceram. Soc. 80 (1997) 3157.
[13] Z.S. Wang, H. Kawauchi, T. Kashima, H. Arakawa, Coord. Chem. Rev. 248 (2004) 1381.
[14] S. Hore, C. Vetter, R. Kern, H. Smit, A. Hinsch, Sol. Energy Mater. Sol. Cells 90 (2006) 1176.
[15] L. Yang, Y. Lin, J. Jia, X. Xiao, X. Li, X. Zhou, J. Power Sources 182 (2008) 370.
[16] W. Yang, F. Wan, Y. Wang, C. Jiang, Appl. Phys. Lett. 95 (2009) 133121.
[17] A.G. Agrios, L. Cesar, P. Comte, M.K. Nazeeruddin, M. Grätzel, Chem. Mater. 18 (2006) 5395.
[18] H.W. Chen, C.Y. Hsu, J.G. Chen, K.M. Lee, C.C. Wang, K.C. Huang, K.C. Ho, J. Power Sources 195 (2010) 6225.
[19] L. Zhao, J.G. Yu, J.J. Fan, P.C. Zhai, S.M. Wang, Electrochem. Commun. 11 (2009) 2052.
[20] K.J. Kim, K.D. Benkstein, J. Lagemaat, A.J. Frank, Chem. Mater. 14 (2002) 1042.
[21] B. Liu, E.S. Aydil, J. Am. Chem. Soc. 131 (2009) 3985.
[22] M.L. Hitchman, F. Tian, J. Electroanal. Chem. 538–539 (2002) 165.
[23] A. Brudnik, A. Gorzkowska-Sobaš, E. Pamula, M. Radecka, K. Zakrzewska, J. Power Sources 173 (2007) 774.
[24] C. Quiñonez, W. Vallejo, G. Gordillo, Appl. Surf. Sci. 256 (2010) 4065.
[25] M. Yan, F. Chen, J. Zhang, M. Anpo, J. Phys. Chem. B 109 (2005) 8673.